A new formalism for the paramagnetic spin susceptibility of metals using relativistic spin-polarized multiple-scattering theory: a temperature-dependent anisotropy effect

1990 J. Phys.: Condens. Matter 2 8365

(http://iopscience.iop.org/0953-8984/2/42/014)

J. Phys.: Condens. Matter 2 (1990) 8365–8379. Printed in the UK

A new formalism for the paramagnetic spin susceptibility of metals using relativistic spin-polarized multiple-scattering theory: a temperature-dependent anisotropy effect

M Matsumoto†§, J B Staunton† and P Strange‡

† Department of Physics, University of Warwick, Coventry CV4 7AL, UK
‡ Department of Physics, University of Keele, Keele ST5 5BG, UK

Received 17 April 1990

Abstract. A new formalism for the static paramagnetic spin susceptibility of metals is given which includes a directional dependence on the magnetic response. This approach leads to an anisotropic generalized Stoner condition. We applied this theory to HCP and FCC cobalt. The starting point was the fully relativistic band structures and densities of states of both phases. The calculated susceptibilities show that an anisotropy appears in the HCP phase, but is absent for the FCC phase within this linear response theory. We also find a temperature dependence of this anisotropy. At low temperatures (< 2500 K) the easy axis is along the c axis whereas at higher temperatures it lies in the ab plane.

1. Introduction

Recently, magnetic anisotropic effects have been investigated using a first principles theory in which both fully relativistic and spin-polarized effects are treated on an equal footing [1–4]. Even for light elements, this approach is necessary for the study of magnetic anisotropy because of the important role of spin–orbit coupling. There are some studies of the magnetic anisotropy of cubic systems [5, 6] using this theoretical framework. Although magnetocrystalline anisotropy effects are likely to be more important in non-cubic systems, there are few theoretical calculations.

The magnetic susceptibility has been calculated by many authors with various methods. We do not include here a complete review of the literature in this field but only refer to those papers which are related to our work. A review is provided in reference [7]. Vosko and Perdew [8] and MacDonald and Vosko [9] obtained a expression for the static paramagnetic spin susceptibility based upon the spin-density functional theory [10]. Stenzel and Winter [7] and Winter *et al* [11] set up a scheme for calculating the dynamic spin susceptibility of metals using a spin-polarized multiple-scattering framework. Staunton *et al* [12] calculated the static susceptibility for Fe and Ni within the disordered local moment picture. These are all non-relativistic calculations. (MacDonald and Vosko incorporated some relativistic effects approximately.)

In this paper we present a new formalism for the static paramagnetic spin susceptibility which corresponds to the relativistic generalization of Stenzel and Winter's

§ Permanent address: University of Library and Information Science, Tsukuba 305, Japan.

0953-8984/90/428365+15$03.50

work. A spatial dependence to the magnetic response is found. In particular we find a generalized Stoner condition which determines the direction along which the magnetization grows as the paramagnetic/ferromagnetic phase transition is crossed. The work is based upon a fully relativistic multiple-scattering (KKR) theory and the local spin-density functional formalism. Temperature dependence is also incorporated by temperature Green function techniques. Although we show here a static spin susceptibility formalism, it is clear that it can be later extended to include dynamic effects. For example the gaps in the spin-wave spectra and the coupling of spin wave excitations to crystallographic directions can be studied. Furthermore as a first step for the study of the magnetic anisotropy of non-cubic systems, the calculation of the homogeneous susceptibility which we give in this paper can be viewed as a complementary approach to magnetic anisotropy energy calculations.

We have applied this formalism to cobalt as a first example. It is a transition metal which is ferromagnetic in the non-cubic HCP as well as in the cubic FCC structural phase. The orbital component of the magnetic properties is also likely to be rather small making it a suitable system to study initially. Eventually it will be worthwhile to extend this work to rare-earth materials, many of which have HCP phases. Consequently it makes sense to apply our theory to a HCP material as well as a cubic one. Tackling rare-earth materials will be a much more difficult task—f electrons must be accounted for as well as s, p and d and orbital effects are also important.

It is well known that ferromagnetic HCP cobalt is stable up to a temperature of 675 K. Above this temperature it passes into a FCC phase, becoming a paramagnet at temperatures greater than 1390 K [13]. In this paper we investigate the magnetic instability and its spatial anisotropy by calculating the static paramagnetic spin susceptibility for Co in both phases.

Underlying our analysis of the susceptibility of cobalt is the band structure. Several band calculations have been carried out for both HCP and FCC cobalt and ours are consistent with them. For HCP Co, early band structure calculations were performed by Hodges and Ehrenreich [14] and Wong *et al* [15]. Then Wakoh and Yamashita [16], Ishida [17] and Batallan *et al* [18]. calculated majority and minority states by using a rigid exchange model. Recently, Matsumoto *et al* [19] calculated a spin-polarized self-consistent (SCF) band structure and compared the theoretical momentum densities with experimental data of the magnetic Compton profiles obtained by Timms *et al* [20]. Strange *et al* [21] obtained relativistic spin-polarized band structures with the magnetization lying along both the *c* and *a* axes.

For FCC Co, Ishida [17] calculated a density of states (DOS) curve for this phase and obtained a very similar DOS curve to that of the HCP phase. Moruzzi *et al* [22] also calculated the band structure and related properties of FCC Co in their series of calculations.

The static paramagnetic spin susceptibility of cobalt has been calculated by Gunnarsson [23]. Local spin-density functional theory was used to modernize the Stoner model, and the results were produced from various band calculations. Shimizu [24] also studied the temperature dependence of the spin susceptibility of FCC cobalt phenomenologically using model DOS curves. A useful review of magnetism in Fe, Ni and Co is given by Wohlfarth [25].

In the next section, following a brief introduction to relativistic density functional theory and multiple-scattering theory, a new formalism of susceptibility is given. We discuss the calculational method in section 3. Some calculations with interpretations are presented in section 4. Finally we draw some conclusions in section 5.

2. The relativistic generalization of the density functional theory of the paramagnetic, static, spin susceptibility

MacDonald and Vosko [9], Rajagopal [26] developed the current density functional theory for a many-relativistic-electron system in the presence of an external potential and magnetic field. MacDonald and Vosko also used the Gordon decomposition of the current, neglecting orbital (diamagnetic) effects and set up a theory in terms of the charge and 'spin-only' magnetization density only. We base our work on this. An effective one-electron Kohn–Sham–Dirac equation can be written:

$$[c\boldsymbol{\alpha}\cdot\boldsymbol{p}+\beta mc^2+1V^{\mathrm{eff}}[n,\boldsymbol{m}]-\beta\boldsymbol{\sigma}\cdot\boldsymbol{B}^{\mathrm{eff}}[n,\boldsymbol{m}]-\varepsilon_i]\Psi_i(\boldsymbol{r})=0 \tag{1}$$

where $\Psi_i(\boldsymbol{r})$ is a 4-spinor and $\boldsymbol{\alpha},\beta$ are standard Dirac matrices. $\boldsymbol{\sigma}$ are the 4×4 Pauli matrices. The effective magnetic field $\boldsymbol{B}^{\mathrm{eff}}[n,\boldsymbol{m}]$ is given by

$$\boldsymbol{B}^{\mathrm{eff}}[n,\boldsymbol{m}]=\mu_{\mathrm{B}}(\boldsymbol{B}^{\mathrm{ext}}(r)-B^{\mathrm{xc}}[n,\boldsymbol{m}]\boldsymbol{m}) \tag{2}$$

and couple to the 'spin-only' part of the current $B^{\mathrm{xc}}[n,\boldsymbol{m}]$ is obtained in the local spin-density functional approximation [23].

$$B^{\mathrm{xc}}[n,\boldsymbol{m}]\sim B^{\mathrm{xc}}(r)=-\frac{r_{\mathrm{s}}^2}{3\pi\mu_{\mathrm{B}}}\left(\frac{2\pi}{3}\right)^{1/3}\delta(r_{\mathrm{s}})\,|\Phi_{\mathrm{d}}(r;\varepsilon_{\mathrm{F}})|^2 \tag{3}$$

where $\delta(r_{\mathrm{s}})$ is the appropriate exchange–correlation parameter. We used the expression given by Gunnarsson and Lundqvist [27], i.e. $\delta(r_{\mathrm{s}})=1-0.036r_{\mathrm{s}}-1.36r_{\mathrm{s}}/(1+10r_{\mathrm{s}})$, r_{s} is the usual parameter of density, defined by $r_{\mathrm{s}}=(3/4\pi n)^{1/3}$ where n is the electronic density. $\Phi_{\mathrm{d}}(r)$ is a relativistic radial wavefunction for d electrons; $|\Phi_{\mathrm{d}}(r)|^2=[|\Phi_2^{3/2}(r)|^2+|\Phi_2^{5/2}(r)|^2]/2$, where the superscripts denote the value of the total angular momentum, j. The function of $B^{\mathrm{xc}}(r)$ for HCP and FCC Co is shown in figure 1. In this figure, the full curve indicates $B^{\mathrm{xc}}(r)$ for HCP Co and the broken curve indicates that of FCC. The difference between the two quantities is small, but not negligible.

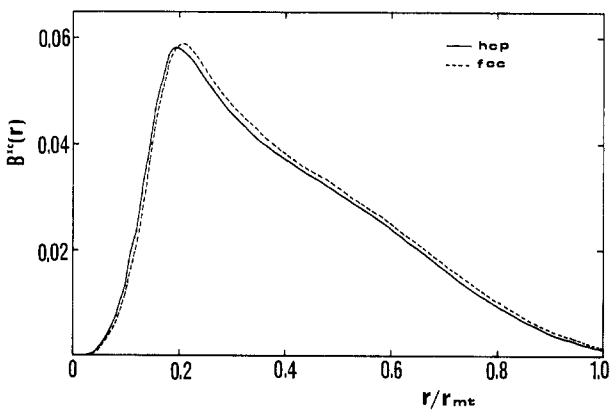

Figure 1. The exchange–correlation function $B^{\mathrm{xc}}(r)$ as a function of r/r_{mt}, where r_{mt} is a radius of the muffin-tin sphere.

We now consider a paramagnetic system which is subjected to a small external magnetic field and determine the response of the system. In the linear response theory, a Green function solution of the integral equation corresponding to (1) is given by

$$G(\boldsymbol{r}_i,\boldsymbol{r}_i;\varepsilon) = G_0(\boldsymbol{r}_i,\boldsymbol{r}_i;\varepsilon) - \sum_j \int G_0(\boldsymbol{r}_i,\boldsymbol{r}'_j;\varepsilon)\beta\boldsymbol{\sigma}\cdot\boldsymbol{B}^{\mathrm{eff}}(\boldsymbol{r}'_j)G_0(\boldsymbol{r}'_j,\boldsymbol{r}_i;\varepsilon)\,\mathrm{d}\boldsymbol{r}'_j. \tag{4}$$

Where G_0 is the Green function of the paramagnetic system, i.e. with zero effective magnetic field $\boldsymbol{B}^{\mathrm{eff}}$. This function is defined in the following way [28]:

$$G_0(\boldsymbol{r}_i,\boldsymbol{r}'_j;\varepsilon) = \begin{cases} \sum_{kk'} Z_k(\boldsymbol{r}_i;\varepsilon)\tau^{ii}_{kk'}(\varepsilon)Z^{\dagger}_{k'}(\boldsymbol{r}'_i;\varepsilon) - \sum_k Z_k(\boldsymbol{r}_i;\varepsilon)J^{\dagger}_k(\boldsymbol{r}'_i;\varepsilon)\theta(r'_i - r_i) \\ \quad - \sum_k J_k(\boldsymbol{r}_i;\varepsilon)Z^{\dagger}_k(\boldsymbol{r}'_i;\varepsilon)\theta(r_i - r'_i) & \text{for } i = j \\ \sum_{kk'} Z_k(\boldsymbol{r}_i;\varepsilon)\tau^{ij}_{kk'}(\varepsilon)Z^{\dagger}_{k'}(\boldsymbol{r}'_j;\varepsilon) & \text{for } i \neq j \end{cases} \tag{5}$$

where the index k describes the two quantum numbers (κ, m_j). κ and m_j are the eigenvalues of the angular momentum operator $\hat{K} = (\hat{\sigma}\cdot\hat{L} + 1)$ and the total angular momentum operator $\hat{J}_z$ respectively. Z_k and J_k are the regular and irregular solutions of the Kohn–Sham–Dirac equation. $\tau^{ij}_{kk'}(\varepsilon)$ is the scattering path operator for the system between lattice sites i and j, introduced by Gyorffy and Stott [29] and defined by

$$\tau^{ij}_{kk'}(\varepsilon) = \frac{1}{\Omega_{\mathrm{BZ}}}\int (t^{-1} - G_0(\boldsymbol{q},\varepsilon))^{-1}_{kk'}\,\mathrm{e}^{\mathrm{i}\boldsymbol{q}\cdot(\boldsymbol{R}_i - \boldsymbol{R}_j)}\mathrm{d}\boldsymbol{q} \tag{6}$$

t is a relativistic single-site t matrix. $G_0(\boldsymbol{q},\varepsilon)$ is the relativistic KKR structure constant [30].

We introduce a rotation operator in spin space which we can use to take into account the spatial dependence of the magnetic field:

$$\boldsymbol{\sigma}\cdot\boldsymbol{B}^{\mathrm{eff}} = \mathrm{Re}\,(\theta,\varphi)\sigma_z\,|\boldsymbol{B}^{\mathrm{eff}}|\,\mathrm{Re}^{\dagger}(\theta,\varphi) \tag{7}$$

where $\mathrm{Re}\,(\theta,\varphi)$ is given by

$$\mathrm{Re}\,(\theta,\varphi) = \begin{pmatrix} (\cos\theta/2)\mathrm{e}^{-\mathrm{i}\varphi/2} & -(\sin\theta/2)\mathrm{e}^{-\mathrm{i}\varphi/2} \\ (\sin\theta/2)\mathrm{e}^{\mathrm{i}\varphi/2} & (\cos\theta/2)\mathrm{e}^{\mathrm{i}\varphi/2} \end{pmatrix}. \tag{8}$$

This matrix is a special case the general form of the Euler rotation matrix. The angles θ,φ describe the orientation of $\boldsymbol{B}^{\mathrm{eff}}$ with respect to the crystal axes.

The magnetic moment $\boldsymbol{m}(\boldsymbol{r})$ is given by

$$\boldsymbol{m}(\boldsymbol{r}_i) = -\frac{1}{\pi}\,\mathrm{tr}\,\beta\boldsymbol{\sigma}\,\mathrm{Im}\int^{\varepsilon_{\mathrm{F}}} G(\boldsymbol{r}_i,\boldsymbol{r}_i;\varepsilon)\,\mathrm{d}\varepsilon \tag{9}$$

where the trace is over spin space. Finally, (4), (5) and (7) are substituted into (9) and after taking the appropriate lattice Fourier transform of the τ matrix, we obtain the following expression

$$m = \int^{r_{\mathrm{mt}}} m(\boldsymbol{r}_i)\,\mathrm{d}\boldsymbol{r}_i = \chi^s_0(\theta,\varphi)B^{\mathrm{ext}} + I\chi^s_0(\theta,\varphi)m \tag{10}$$

where

$$\chi_0^s(\theta,\varphi) = \frac{\mu_B^2}{\pi}\,\mathrm{Im}\int f(\varepsilon-\nu)\,\mathrm{d}\varepsilon\Bigg(\sum_{kk'k''k'''}\delta_{ll'''}\delta_{l'l''}g^{kk'''}_{k''k'}(\theta,\varphi)U_{kk'''}(\varepsilon)U_{k''k'}(\varepsilon)$$
$$\times\frac{1}{\Omega_{BZ}}\sum_{s'}\int\tau_{kk'ss'}(\varepsilon;\boldsymbol{q})\tau_{k''k'''s's}(\varepsilon;\boldsymbol{q})\,\mathrm{d}\boldsymbol{q}$$
$$-\sum_{kk'k''}\delta_{ll''}\delta_{l'l''}(g^{kk''}_{k''k'}(\theta,\varphi)+g^{k''k}_{k'k''}(\theta,\varphi))$$
$$\times(\Gamma_{kk''k'}(\varepsilon)+\Gamma^*_{k'k''k}(\varepsilon))\frac{1}{\Omega_{BZ}}\int\tau_{kk'ss}(\varepsilon;\boldsymbol{q})\,\mathrm{d}\boldsymbol{q}\Bigg) \tag{11}$$

and

$$I\chi_0^s(\theta,\varphi) = -\frac{\mu_B^2}{\pi}\,\mathrm{Im}\int f(\varepsilon-\nu)\,\mathrm{d}\varepsilon\Bigg(\sum_{kk'k''k'''}\delta_{ll'''}\delta_{l'l''}g^{kk'''}_{k''k'}(\theta,\varphi)U_{kk'''}(\varepsilon)UP_{k''k'}(\varepsilon)$$
$$\times\frac{1}{\Omega_{BZ}}\sum_{s'}\int\tau_{kk'ss'}(\varepsilon;\boldsymbol{q})\tau_{k''k'''s's}(\varepsilon;\boldsymbol{q})\,\mathrm{d}\boldsymbol{q}$$
$$-\sum_{kk'k''}\delta_{ll''}\delta_{l'l''}[g^{kk''}_{k''k'}(\theta,\varphi)(\Gamma P_{kk''k'}(\varepsilon)+P\Gamma^*_{k'k''k}(\varepsilon))$$
$$+g^{k''k}_{k'k''}(\theta,\varphi)(P\Gamma_{kk''k'}(\varepsilon)+\Gamma P^*_{k'k''k}(\varepsilon))]\frac{1}{\Omega_{BZ}}\int\tau_{kk'ss}(\varepsilon;\boldsymbol{q})\,\mathrm{d}\boldsymbol{q}\Bigg). \tag{12}$$

The index s denotes the position of an atom in the unit cell. $f(\varepsilon-\nu)$ is Fermi–Dirac distribution function and ν is the chemical potential. $g^{kk'}_{k''k'''}(\theta,\varphi)$ is given in terms of Clebsch–Gordan coefficients as follows;

$$g^{kk'}_{k''k'''}(\theta,\varphi) = (\cos\theta\, g^{m_j}_{kk'} + \sin\theta\, h^{m_jm'_j}_{kk'})(\cos\theta\, g^{m''_j}_{k''k'''} + \sin\theta\, h^{m''_jm'''_j}_{k''k'''}) \tag{13}$$

and

$$g^{m_j}_{kk'} = C^{\uparrow,m_j-\uparrow}_{\kappa,m_j}C^{\uparrow,m_j-\uparrow}_{\kappa',m_j} - C^{\downarrow,m_j-\downarrow}_{\kappa,m_j}C^{\downarrow,m_j-\downarrow}_{\kappa',m_j}$$
$$h^{m_jm'_j}_{kk'} = \mathrm{e}^{\mathrm{i}\varphi}\,C^{\uparrow,m_j-\uparrow}_{\kappa',m_j}C^{\downarrow,m'_j-\downarrow}_{\kappa',m'_j}\delta_{m_j-1/2,m'_j+1/2} + \mathrm{e}^{-\mathrm{i}\varphi}C^{\downarrow,m_j-\downarrow}_{\kappa,m_j}C^{\uparrow,m'_j-\uparrow}_{\kappa',m'_j}\delta_{m_j+1/2,m'_j-1/2} \tag{14}$$

and

$$U_{kk'}(\varepsilon) = \int^{r_{mt}} R_k(r;\varepsilon)R^*_{k'}(r;\varepsilon)r^2\,\mathrm{d}r$$
$$\Gamma_{kk'k''}(\varepsilon) = \int^{r_{mt}} R_k(r;\varepsilon)Q^*_{k'}(r;\varepsilon)[\int_0^r R_{k'}(r';\varepsilon)R^*_{k''}(r';\varepsilon)r'^2\,\mathrm{d}r']r^2\,\mathrm{d}r$$
$$UP_{kk'}(\varepsilon) = \int^{r_{mt}} R_k(r;\varepsilon)B^{xc}(r)R^*_{k'}(r;\varepsilon)r^2\,\mathrm{d}r \tag{15}$$
$$\Gamma P_{kk'k''}(\varepsilon) = \int^{r_{mt}} R_k(r;\varepsilon)Q^*_{k'}(r;\varepsilon)[\int_0^r R_{k'}(r';\varepsilon)B^{xc}(r')R^*_{k''}(r';\varepsilon)r'^2\,\mathrm{d}r']r^2\,\mathrm{d}r$$
$$P\Gamma_{kk'k''}(\varepsilon) = \int^{r_{mt}} R_k(r;\varepsilon)B^{xc}(r)Q_{k'}(r;\varepsilon)[\int_0^r R_{k'}(r';\varepsilon)R^*_{k''}(r';\varepsilon)r'^2\,\mathrm{d}r']r^2\,\mathrm{d}r.$$

In general, the regular solution $R_k(r)$ and the irregular one $Q_k(r)$ of the Kohn–Sham–Dirac radial equation are real functions when the energy is itself real valued. When the energy is extended to complex values, as used later, these values also become complex.

A temperature Green function is introduced on taking into account the temperature dependence [31]. This is done by the following transformation (see, for example, [32]):

$$\mathrm{Im}\int G(\varepsilon)\frac{\mathrm{d}\varepsilon}{\pi}f(\varepsilon-\nu)\rightarrow -2k_{\mathrm{B}}T\,\mathrm{Re}\sum_{n>0}G(\nu+\mathrm{i}\omega_n) \tag{16}$$

where ω_n is Matsubara frequency, defined by $\omega_n=(2n+1)\pi k_{\mathrm{B}}T$, k_{B} is Boltzman constant and T is the temperature. Unfortunately, the convergence of this summation over the Matsubara frequencies is very slow, and we use the technique introduced by Staunton *et al* [12] to avoid this difficulty. This technique is as follows:

$$\begin{aligned}2k_{\mathrm{B}}T\,\mathrm{Re}\sum_n\frac{1}{\Omega_{\mathrm{BZ}}}\int\tau_{kk'}(\nu+\mathrm{i}\omega_n;\boldsymbol{q})\,\mathrm{d}\boldsymbol{q}&\\ =2k_{\mathrm{B}}T\,\mathrm{Re}\sum_n\Bigl(\frac{1}{\Omega_{\mathrm{BZ}}}\int\tau_{kk'}(\nu+\mathrm{i}\omega_n;\boldsymbol{q})\,\mathrm{d}\boldsymbol{q}&\\ -t_k(\nu+\mathrm{i}\omega_n)\delta_{kk'}\Bigr)-\frac{1}{\pi}\mathrm{Im}\int t_k(\varepsilon)f(\nu-\varepsilon)\,\mathrm{d}\varepsilon&\end{aligned} \tag{17}$$

i.e. part of the calculation is carried out in the complex plane and part on the real axis. At large Matsubara frequencies, τ approximates to the single-site t matrix. In practice, when $\omega_n>1$ Ryd the term from the Matsubara sum is essentially zero. The remaining term involving the single-site t matrix integral is easy to calculate.

Consequently, we get a formula for the spin paramagnetic susceptibility.

$$\chi=\frac{\boldsymbol{m}}{\boldsymbol{B}}=\frac{\chi_0(\theta,\varphi,T)}{1-I\chi_0(\theta,\varphi,T)} \tag{18}$$

and if the stoner condition

$$1-I\chi_0(\theta,\varphi,T)<1 \tag{19}$$

is satisfed, the system is ferromagnetic, where

$$\begin{aligned}\chi_0(\theta,\varphi,T)=-2k_{\mathrm{B}}T\mu_{\mathrm{B}}^2\sum_{n>0}\sum_{s'}\mathrm{Re}\Bigl[\sum_{kk'k''k'''}\delta_{ll'''}\delta_{l'l'''}g_{k''k'}^{kk'''}(\theta,\varphi)&\\ \times U_{kk'''}(\nu+\mathrm{i}\omega_n)U_{k''k'}(\nu+\mathrm{i}\omega_n)&\\ \times\Bigl(\frac{1}{\Omega_{\mathrm{BZ}}}\int\tau_{kk's's'}(\nu+\mathrm{i}\omega_n;\boldsymbol{q})\tau_{k''k'''s's}(\nu+\mathrm{i}\omega_n;\boldsymbol{q})\,\mathrm{d}\boldsymbol{q}&\\ -t_k(\nu+\mathrm{i}\omega_n)t_{k''}(\nu+\mathrm{i}\omega_n)\delta_{ss'}\delta_{kk'}\delta_{k''k'''}\Bigr)&\\ -\sum_{kk'k''}\delta_{ll''}\delta_{l'l'''}(g_{k''k'}^{kk''}(\theta,\varphi)+g_{k'k''}^{k''k}(\theta,\varphi))(\Gamma_{kk''k'}(\nu+\mathrm{i}\omega_n)+\Gamma_{k'k''k}^{*}(\nu+\mathrm{i}\omega_n))&\end{aligned}$$

$$\times \left(\frac{1}{\Omega_{\mathrm{BZ}}} \int \tau_{kk's s}(\nu + \mathrm{i}\omega_n; \boldsymbol{q})\, \mathrm{d}\boldsymbol{q} - t_k(\nu + \mathrm{i}\omega_n)\delta_{kk'} \right) \Bigg]$$

$$+ \frac{\mu_{\mathrm{B}}^2}{\pi} \mathrm{Im} \sum_{kk'} \delta_{ll'} \int f(\varepsilon - \nu) g_{k'k}^{kk'}(\theta, \varphi) [U_{kk'}^2(\varepsilon) t_k(\varepsilon) t_{k'}(\varepsilon)$$

$$- (2\Gamma_{kk'k}(\varepsilon) t_k(\varepsilon) + 2\Gamma_{k'kk'}(\varepsilon) t_{k'}(\varepsilon))]\, \mathrm{d}\varepsilon \tag{20}$$

and

$$I\chi_0(\theta, \varphi, T) = 2k_{\mathrm{B}} T \mu_{\mathrm{B}}^2 \sum_{n>0} \sum_{s'} \mathrm{Re} \Bigg[\sum_{kk'k''k'''} \delta_{ll'''} \delta_{l'l''} g_{k''k'}^{kk'''}(\theta, \varphi)$$

$$\times U_{kk'''}(\nu + \mathrm{i}\omega_n) U P_{k''k'}(\nu + \mathrm{i}\omega_n)$$

$$\times \left(\frac{1}{\Omega_{\mathrm{BZ}}} \int \tau_{kk's s'}(\nu + \mathrm{i}\omega_n; \boldsymbol{q}) \tau_{k''k'''s's}(\nu + \mathrm{i}\omega_n; \boldsymbol{q})\, \mathrm{d}\boldsymbol{q} \right.$$

$$\left. - t_k(\nu + \mathrm{i}\omega_n) t_{k''}(\nu + \mathrm{i}\omega_n) \delta_{ss'} \delta_{kk'} \delta_{k''k'''} \right)$$

$$- \sum_{kk'k''} \delta_{ll''} \delta_{l'l'''} [g_{k''k'}^{kk''}(\theta, \varphi)(\Gamma P_{kk''k'}(\nu + \mathrm{i}\omega_n) + P\Gamma_{k'k''k}^{*}(\nu + \mathrm{i}\omega_n))$$

$$+ g_{k'k''}^{k''k}(\theta, \varphi)(P\Gamma_{kk''k'}(\nu + \mathrm{i}\omega_n) + \Gamma P_{k'k''k}^{*}(\nu + \mathrm{i}\omega_n))]$$

$$\times \left(\frac{1}{\Omega_{\mathrm{BZ}}} \int \tau_{kk's s}(\nu + \mathrm{i}\omega_n; \boldsymbol{q})\, \mathrm{d}\boldsymbol{q} - t_k(\nu + \mathrm{i}\omega_n)\delta_{kk'} \right) \Bigg]$$

$$- \frac{\mu_{\mathrm{B}}^2}{\pi} \mathrm{Im} \sum_{kk'} \delta_{ll'} \int f(\varepsilon - \nu) g_{k'k}^{kk'}(\theta, \varphi) [U_{kk'}(\varepsilon) U P_{kk'}(\varepsilon) t_k(\varepsilon) t_{k'}(\varepsilon)$$

$$- (\Gamma P_{kk'k}(\varepsilon) + P\Gamma_{kk'k}(\varepsilon)) t_k(\varepsilon) + (P\Gamma_{k'kk'}(\varepsilon) + \Gamma P_{k'kk'}(\varepsilon)) t_{k'}(\varepsilon)]\, \mathrm{d}\varepsilon \tag{21}$$

From (18), we can see that this equation has the form of a Stoner-type susceptibility formula. A corresponding Stoner enhancement factor I is obtained by a ratio of equation (21) to equation (20). We call this quantity the generalized Stoner parameter. It is important to note that the expressions (18)–(21) depend on not only temperature but also on the direction along which the magnetization is being introduced. This direction is given by angles θ and φ.

3. Calculations

Equations (20) and (21) require the evaluation of an integral over the Brillouin zone (BZ). This integral, particularly for non-cubic systems, is computationally demanding. There are two main reasons: the τ matrix has many singular points on the real energy axis (i.e. where the KKR condition is satisfied). These singular points are avoided by performing the energy integration in the complex plane. This becomes a Matsubara frequency summation. For small Matsubara frequencies, however, the τ matrix still varies rapidly along various directions $\boldsymbol{q}$. The second reason is the large number of elements of the integrand. A Brillouin zone integral must be carried out

for every (κ, m_j, s) element. For example, there are two atoms in the unit cell for the HCP structure and taking into account κ, m_j values which include orbital angular momentum values ≤ 2, the τ matrix has 36×36 elements. Furthermore, in the case of the $\tau \times \tau$ of equations (20) and (21), the number of elements is now 36^4. Excessive CPU time is required if we are to calculate the BZ integral for every element. By exploiting a symmetry properties of the τ matrix, however, this difficulty can be avoided. The summation over s is carried out before the BZ integral and those elements which are zero by symmetry are ignored. In this way, the number of elements is reduced to manageable proportions. For instance, it is reduced to 36 elements from 36×36 (τ) and to 8581 from 36^4 ($\tau \times \tau$) for HCP.

We carried out the BZ integration using the prism method [33]. For the irreducible zone of the HCP and FCC BZ, we chose 38 and 36 prisms respectively. Each prism was divided into 16–42 planes between an origin and an edge of the prism. As mentioned early in this section, for small Matsubara frequencies, many divisions are used. On the other hand, for large frequencies, fewer are needed. The number used depends upon the energy values. In table 1, tests of the convergence of this integral with respect to energy and divisions are shown. The integrand is $\tau(\nu + i\omega_n)$ and the integration is taken over only one prism. The tabulated values show a ratio with the value achieved using 95 divisions. As is seen from this table, sufficient accuracy is achieved with just 16 divisions for Im(energy;ε) = 0.05 Ryd. On the other hand, for the case of Im(ε) = 0.005 Ryd, more than 42 divisions are needed for the same accuracy. Strictly the integral of $\tau \times \tau$ requires a great number of divisions per prism, The expense, in terms of computer resources of using many more divisions is not justified nor necessary, since it is the Matsubara sum of these terms which is the important quantity.

Table 1. Convergence with respect to the number of divisions (ND) for one BZ line integral. The results are expressed as ratios with respect to that for 95 divisions.

Im(ε)	ND =	8	16	32	42	95
0.05		0.987	1.000 038	1.000 008	1.000 002	1.0
0.005		0.560	0.704	0.960	0.997 6	1.0

The BZ integration is carried out for an irreducible segment, i.e. 1/24th for HCP and 1/48th for FCC (or cubic) systems. It is summed over the whole BZ by appropriate transformations. Firstly, the κ, m_j representation is transformed to the $lm\sigma$ representation [30]

$$\tau^{\mathrm{1st}}_{LL'\sigma\sigma'} = \sum_{kk'} C^{\sigma, m_j - \sigma\,\dagger}_{\kappa, m_j} \tau^{\mathrm{1st}}_{kk'} C^{\sigma', m_j - \sigma'}_{\kappa', m_j} . \tag{22}$$

Secondly, a space symmetry transformation $R^n_{LL'}$ and spin transformation $S^n_{\sigma\sigma'}$ are made. Then an inverse transformation of (22), i.e. $lm\sigma \rightarrow \kappa m_j$ representation, is carried out. Finally, the BZ integral is completed by summing over each segment. In short,

$$\tau^{\mathrm{TOT}}_{KK'} = \sum_{n}^{\mathrm{BZ}} \sum_{\sigma\sigma'} C^{\sigma, m_j - \sigma\,\dagger}_{\kappa, m_j} (S^{n\,\dagger}_{\sigma\sigma''} R^{n\,\dagger}_{LL''} \tau^{\mathrm{1st}}_{L''L'''\sigma''\sigma'''} R^{n}_{L'''L'} S^{n}_{\sigma'''\sigma'}) C^{\sigma', m_j - \sigma'}_{\kappa', m_j} \tag{23}$$

where the spin transformation matrix $S^n_{\sigma\sigma'}$ is written as

$$S^n_{\sigma\sigma'} = \begin{pmatrix} \cos(\beta_n/2)e^{-i(\alpha_n+\gamma_n)/2} & -\sin(\beta_n/2)e^{i(\alpha_n-\gamma_n)/2} \\ \sin(\beta_n/2)e^{i(\gamma_n-\alpha_n)/2} & \cos(\beta_n/2)e^{i(\alpha_n+\gamma_n)/2} \end{pmatrix} \tag{24}$$

α, β, γ are the Eulerian angles (see, for example, [34]).

4. Results and discussion

We obtained SCF muffin-tin potentials for both HCP and FCC paramagnetic cobalt from the non-relativistic APW method. In order to estimate the Fermi energy, we calculated relativistic band structures from these potentials by using a fully relativistic KKR method. Although the input potentials are calculated non-relativistically, this is a reasonable approximation because cobalt is a light element. Relativistic band structures are shown in figure 2, and the density of states (DOS) curves are shown in figure 3.

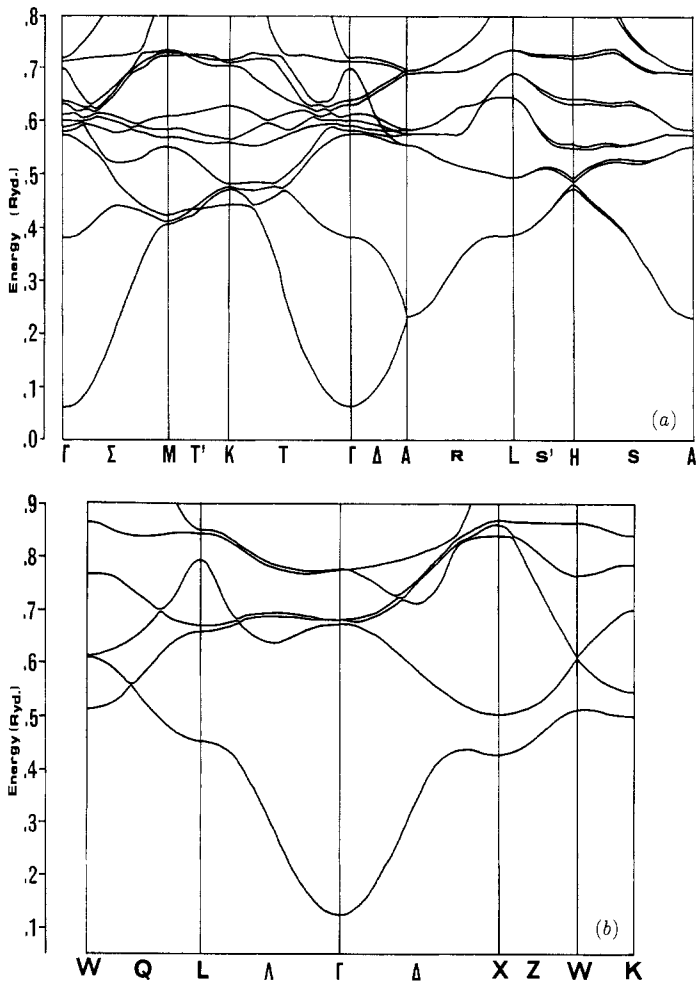

Figure 2. Relativistic band structure, of (*a*) HCP Co and (*b*) FCC Co.

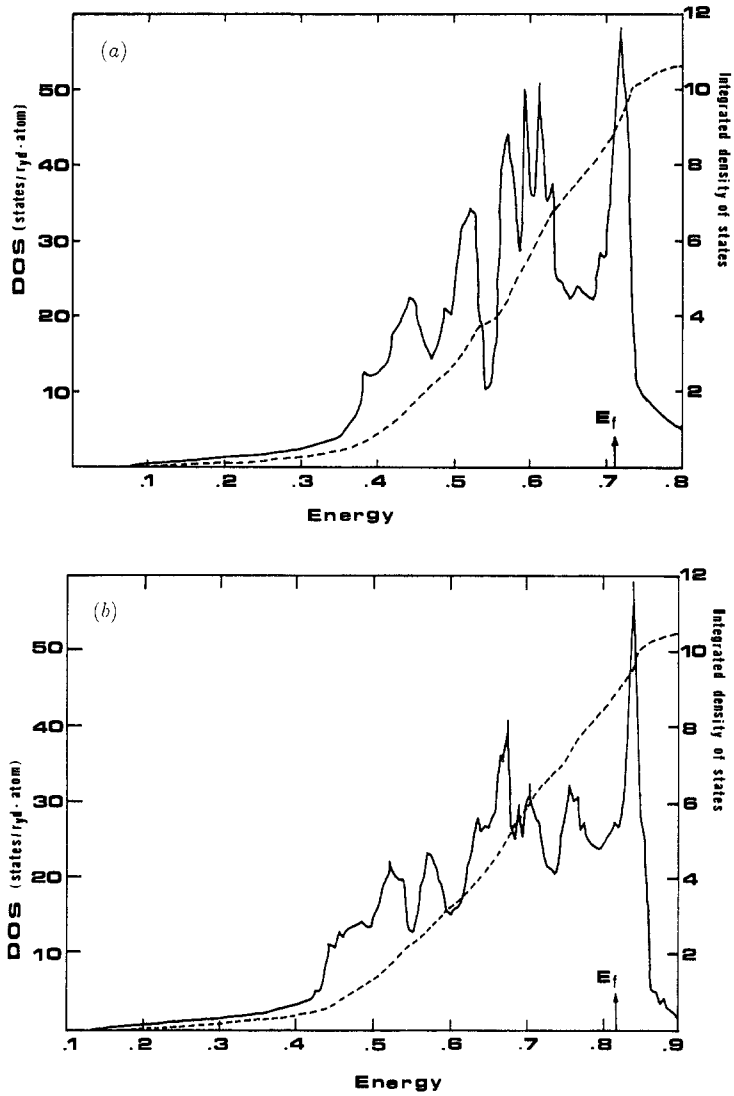

Figure 3. Density of states curve of HCP (*a*) and FCC Co (*b*). Broken curves indicate the integrated density of states (number of states). Arrows show the Fermi energies.

The Fermi energies are 0.711 Ryd (HCP) and 0.819 Ryd (FCC). The DOS at the Fermi energy $N(\varepsilon_F)$ are 46.7 and 27.2 states/Ryd atom for HCP and FCC Co, respectively. These values are consistent with other band calculations. As shown later, we obtained a generalized Stoner-enhancement factor of about 0.037 for both phases. At low temperatures (< 4345 K) the calculated susceptibility from (18)–(21) is negative, for HCP Co, indicating that this system is ferromagnetic. FCC Co also produces a negative-valued susceptibility but of smaller magnitude suggesting that this system is close to the para/ferromagnetic crossover. In fact, the non-relativistic results of Moruzzi *et al* find FCC Co to be paramagnetic (their results are $N(\varepsilon_F) = 27.3$ states/Ryd atom and $I = 0.036$ [22]). Figure 4 shows the inverse susceptibility as a function of temperature. The transition temperatures are 4345 K and 2295 K for

HCP and FCC Co respectively. As expected, these values are too high compared with experimental values (1388 K, FCC [13]). In general, it is insufficient to take into account only Stoner excitations for estimates of the Curie temperature and the behaviour of metals at finite temperatures. It is necessary to include spin-wave excitations, a magnon–electron interaction and a spin fluctuation effects [35, 36].

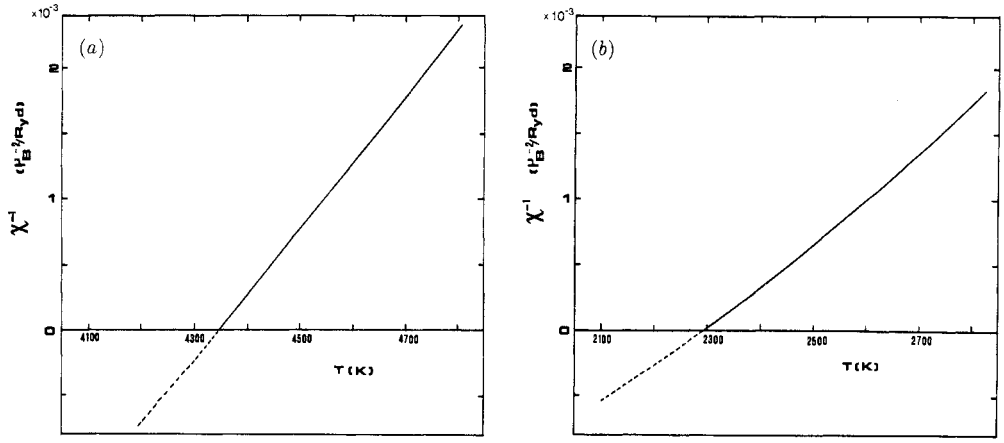

Figure 4. The inverse of the paramagnetic spin susceptibility as a function of temperature (a) for HCP Co, (b) for FCC Co.

We show a temperature derivative of the inverse susceptiblity $d\chi^{-1}/dT$ for FCC Co in figure 5. If χ follows a Curie–Weiss law exactly, this quantity should be constant with changing temperature. A deviation from the Curie–Weiss law is observed experimentally [37]. Coincidentally the temperature derivative curve which we found is also not constant. If we follow the same sort of analysis as Shimizu [24], the deviation from Curie–Weiss behaviour is smaller than that found experimentally.

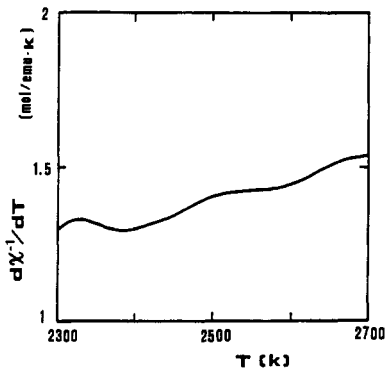

Figure 5. The temperature derivative of the inverse susceptibility, $d\chi^{-1}/dT$ for FCC Co.

The temperature dependence of the unenhanced susceptibility is shown in figure 6. The generalized Stoner enhancement factor I which is obtained by $I(T) = I\chi_0(T)/\chi_0(T)$, is also shown in this figure. The factor $I(T)$ depends on temperature,

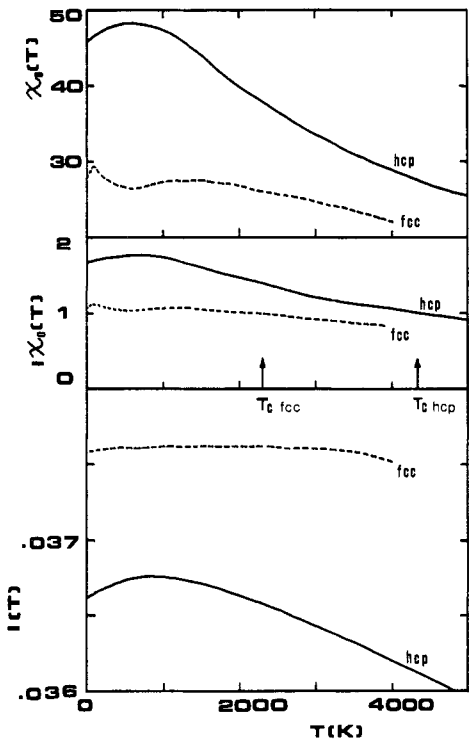

Figure 6. Temperature dependence $\chi_0(T)$, $I\chi_0(T)$ and the generalized enhancement factor $I(T)$. The full curves are for HCP Co and the broken curves for FCC Co.

but the effect is very small. The temperature dependence of I for HCP Co is larger than that for FCC Co and the difference between the maximum and minimum values, ΔI, is 0.0008 for this temperature range. Averaged values of I are about 0.0376 for FCC and 0.0365 for HCP. There is a difference of about 0.001 between FCC and HCP Co. It seems that this is due to the difference between the exchange–correlation functions as shown in figure 1. Although this difference is small, it is very important in the Stoner condition (19). Because, in the case of FCC Co, if value of I is 0.0365, the Stoner condition (19) is not satisfied.

A spatial dependence of $I\chi_0$ on HCP Co is shown in figure 7(a). On the vertical axis is the value of $[I\chi_0(\theta,\varphi)/I\chi_0(\theta=0,\varphi=0)-1]$. A ferromagnetic state is stable when this value has its largest value at particular angles θ and φ. The magnetization thus grows along the direction defined by these angles θ,φ. Our results suggest that the easy axis changes with temperature. For instance, the value of this quantity at $T=1600$ K decreases as θ increases from 0° to 90°. This means that $\theta=0°$ (c axis) defines the easy axis. On the other hand, at $T=4600$ K, the value is larger at $\theta=90°$ and this means that the easy axis lies in the ab plane. However, there was no dependence on the angle φ. Moreover, no directional dependence for FCC Co, a cubic system, appeared within the accuracy of these calculations. Magnetic anisotropy is a result of spin–orbit coupling. Our results were obtained from fully relativistic calculations. We did not treat the spin–orbit coupling as a perturbation. Nevertheless, no anisotropy effects are evident for cubic systems and for similar reasons, no distinction between angles within the ab plane for HCP systems can be made. We think that this is inherent

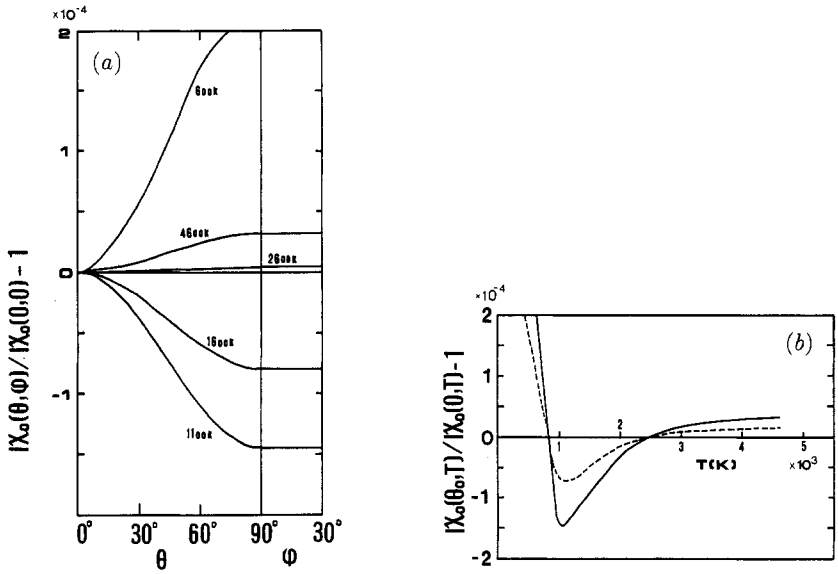

Figure 7. (*a*) shows the angular dependence of $[I\chi_0(\theta,\varphi)/I\chi_0(\theta=0,\varphi=0)-1]$ for HCP Co and (*b*) shows the the temperature dependence of the same quantity.

in the linear response formalism for the cubic systems. In order to confirm this, we evaluated the contribution to the susceptibility from one Matsubara frequency (see equations (20) and (21)) for a heavy element with cubic structure, in which spin–orbit coupling effects are large. No anisotropy effects were found here either. This means that the absence of anisotropy effects arises from the symmetry properties of the τ and $\tau \times \tau$ matrices, and does not depend on their numerical values. It seems to indicate that a fully relativistic linear response version of the paramagnetic spin susceptibility is isotropic for the cubic systems.

Fig 7(*b*) shows the temperature dependence of the anisotropy effects found for HCP Co. As shown in this figure, the easy axis is the *c* axis below a temperature of $T = 2500$ K, but this easy axis changes into the *ab* plane above this temperature. A full curve indicates the result for $\theta = 90°$ and a broken curve indicates that of $\theta = 45°$. Unfortunately, there is no experimental evidence to support our results, because HCP Co is structurally unstable in this temperature range (melting point = 1765 K). But the temperature dependence of the magnetocrystalline anisotropy constants have been observed by several authors [38–40]. Their results showed the *c* axis ceases to be the easy axis above about 500 K and the easy axis lies along a cone of semivertical angle. This indicates that if cobalt would remain in the HCP phase for higher temperatures, then its easy axis might lie within the *ab* plane as it approaches the magnetic phase transition temperature. In figure 7(*b*) the easy axis lies in the *ab* plane below about 800 K. At low temperatures, ferromagnetic HCP cobalt's easy axis lies along the *c* axis. Clearly a complementary calculation of the magnetic anisotropy energy of ferromagnetic HCP cobalt needs to be carried out to complete the picture. This work is in progress.

We should point out that we did not include any temperature dependence to the axial ratio c/a and the chemical potential. These might effect the results. Szpunar and Strange [41] showed with a semi-relativistic band structure calculation that the

magnetic properties change as the axial ratio is varied for HCP Co. Strange *et al* [42] showed that the easy axis changes with axial ratio of iron on a tetragonal lattice. Ono and Maeta [43] also pointed out that the temperature dependence of magnetocrystalline anisotropy in HCP Co has a correlation with the change in the lattice parameter ratio from their experimental studies. The change of the chemical potential with temperature is proportional to the logarithmic derivative of the density of states with energy, which is very large for HCP Co. This temperature dependence of the chemical potential might also affect the anisotropic effects.

The temperature dependence of the anisotropy of the paramagnetic spin susceptibility which we find, is due to Stoner-like excitations which include the effects of spin–orbit coupling. However, as expected this spatial dependence is a very small value. We look forward to calculations of the magnetic anisotropy of HCP cobalt in the ferromagnetic phase which should complement our paramagnetic spin susceptibility calculations.

5. Conclusion

We have given a new formalism for the static paramagnetic spin susceptibility. This formalism includes a dependence upon the spatial direction of the induced magnetization. This is achieved by taking into account fully relativistic and the spin-polarized effects based upon a first principles theory. It can ultimately be extended to include dynamic effects. We applied this theory to both HCP and FCC Co. As expected the estimated Curie temperatures are too high in comparison with experimental values. Spin-wave excitations, magnon–electron interactions and the spin fluctuation effects have been neglected and this is probably the main cause of the discrepancy.

The anisotropy of the susceptibility does not appear for FCC Co. It seems that this is inherent in the fully relativistic linear response formalism for the cubic systems. On the other hand, a temperature dependence of the anisotropy of the susceptibility is obtained for HCP Co. This is a novel result. Unfortunately there are no experimental results for the paramagnetic susceptibility for HCP Co.

There is some small inaccuracy in the low-temperature range due to the numerical calculations in the BZ integral but this does not effect the main findings: an anisotropy of the susceptibility which varies with temperature. We hope to apply this theory to paramagnetic metals for which experimental data are available, in the near future.

Acknowledgments

One of the authors (MM) would like to thank the Science and Engineering Research Council for financial support.

References

[1] Feder R (ed) 1985 *Polarised Electrons in Surface Physics* (Singapore: World Scientific)
[2] Staunton J B, Poulter J, Gyorffy B L and Strange P 1988 *J. Phys. C: Solid State Phys.* **21** 1595
[3] Schadler G, Weinberger P, Boring A M and Albers R C 1987 *Phys. Rev.* B **35** 4324
[4] Strange P, Staunton J B and Gyorffy B L 1984 *J. Phys. C: Solid. State. Phys.* **17** 3355

[5] Strange P, Ebert H, Staunton J B and Gyorffy B L 1989 *J. Phys.: Condens. Matter* **1** 3947
[6] Fritsche L, Noffke J and Eckardt H 1987 *J. Phys. F: Met. Phys.* **17** 943
[7] Stenzel E and Winter H 1985 *J. Phys. F: Met. Phys.* **15** 1571
[8] Vosko S H and Perdew J P 1975 *Can. J. Phys.* **53** 1385
[9] MacDonald A H and Vosko S H 1979 *J. Phys. C: Solid State Phys.* **12** 2977
[10] Kohn W and Sham L J 1965 *Phys. Rev.* 140 A1133
[11] Winter H, Stenzel E, Szotek Z and Temmerman W M 1988 *J. Phys. F: Met. Phys.* **18** 485
[12] Staunton J B, Gyorffy B L, Stocks G M and Wadsworth J 1986 *J. Phys. F: Met. Phys.* **16** 1761
[13] Colvin R V and Araj 1965 *J. Phys. Chem. Solids* **26** 435
[14] Hodges L and Ehrenreich H 1968 *J. Appl. Phys.* **39** 1280
[15] Wong K C, Wohlfarth E P and Hum D M 1969 *Phys. Lett.* **29A** 452
[16] Wakoh S and Yamashita J 1970 *J. Phys. Soc. Japan* **28** 1151
[17] Ishida S 1972 *J. Phys. Soc. Japan* **33** 369
[18] Batallan F, Rosenman I and Sommers C B 1975 *Phys. Rev.* B **11** 545
[19] Matsumoto M, Tomimoto K and Wakoh S 1990 to be submitted
[20] Timms D N, Brahmia A, Collins P, Collins S P, Cooper M J, Holt R S, Kane P P, Clark G and Laundy D 1988 *J. Phys. F: Met. Phys.* **18** L57
[21] Strange P 1988 private communication
[22] Moruzzi V L, Janak J F and Williams A R 1978 *Calculated Electronic Properties of Metals* (Oxford: Pergamon)
[23] Gunnarsson O 1976 *J. Phys. F: Met. Phys.* **6** 587
[24] Shimizu M 1977 *Physica* B **91** 14
[25] Wohlfarth E P 1980 *Ferromagnetic Materials* vol 1, ed E P Wohlfarth (Amsterdam: North-Holland)
[26] Rajagopal A K 1978 *J. Phys. C: Solid State Phys.* **11** L943
[27] Gunnarsson O and Lundqvist B I 1976 *Phys. Rev.* B **13** 4274
[28] Faulkner J S and Stocks G M 1980 *Phys. Rev.* B **21** 3222
[29] Gyorffy B L and Stott M J 1973 *Band Structure Spectroscopy of Metals and Alloys* ed D J Fabian and L M Watson (New York: Academic)
[30] Onodera Y and Okazaki M 1966 *J. Phys. Soc. Japan* **21** 1273
[31] Matsubara T 1955 *Prog. Theor. Phys.* **14** 351
[32] Kirzhnis D A 1967 *Field Theoretical Methods in Many-Body Systems* (Oxford: Pergamon)
[33] Stocks G M, Temmerman W M and Gyorffy B L 1978 *Electrons in Disordered Metals and at Metallic Surfaces (NATO Advanced Study Institutes Series B42)* ed P Phariseau *et al* (New York: Plenum)
[34] Morgan D J 1969 *Solid State Theory* ed P T Lansberg (London: Wiley-Interscience)
[35] Edwards D M 1978 *Proc. Toronto Conf. (Inst. Phys. Conf. Proc. 39)* (Bristol: Institute of Physics)
[36] Moriya T 1977 *Physica* B **86–88** 356, **91** 235
[37] Nakagawa Y 1956 *J. Phys. Soc. Japan* **11** 855
[38] Barnier Y, Pauthenet R and Rimet G 1961 *C. R. Acad. Sci., Paris* **253** 400
[39] Ono F and Yamada O 1979 *J. Phys. Soc. Japan* **46** 462
[40] Paize D M, Szpunar B and Tanner B K 1984 *J. Magn. Magn. Mater.* **44** 239
[41] Szpunar B and Strange P 1985 *J. Phys. F: Met. Phys.* **15** L165
[42] Strange P, Staunton J B and Ebert H 1989 *Europhys. Lett.* **9** 169
[43] Ono F and Maeta H 1989 *Physica* B **161** 134